


AUTHOR QUERY FORM

 ELSEVIER	Journal: JPOL Article Number: 15051	Please e-mail or fax your responses and any corrections to: E-mail: corrections.esco@elsevier.tnq.co.in Fax: +31 2048 52789
--	--	---

Dear Author,

Please check your proof carefully and mark all corrections at the appropriate place in the proof (e.g., by using on-screen annotation in the PDF file) or compile them in a separate list. Note: if you opt to annotate the file with software other than Adobe Reader then please also highlight the appropriate place in the PDF file. To ensure fast publication of your paper please return your corrections within 48 hours.

For correction or revision of any artwork, please consult <http://www.elsevier.com/artworkinstructions>.

Any queries or remarks that have arisen during the processing of your manuscript are listed below and highlighted by flags in the proof.

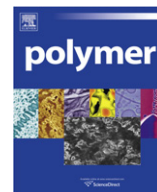
Location in article	Query / Remark: Click on the Q link to find the query's location in text Please insert your reply or correction at the corresponding line in the proof
Q1	Please check the layout of Table 3.
Q2	Please provide caption for scheme 1.
Q3	Please confirm that given names and surnames have been identified correctly.

Thank you for your assistance.



Contents lists available at SciVerse ScienceDirect

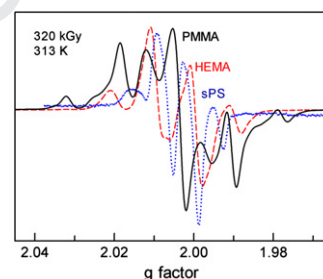
Polymer

journal homepage: www.elsevier.com/locate/polymer

Graphical Abstract

EPR study of radical annihilation kinetics of γ -ray-irradiated acrylic (PMMA) at elevated temperatures

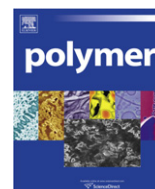
Polymer 2011, ■, ■ ■ ■

J.S. Peng^a, Li-June Ming^b, Young-Shang Lin^a, Sanboh Lee^{a,*}^a Department of Materials Science and Engineering, National Tsing Hua University, 101 Kuang Fu Road, 2nd Sec., Hsinchu 300, Taiwan^b Department of Chemistry, University of South Florida, Tampa, FL 33620-5250, USA



Contents lists available at SciVerse ScienceDirect

Polymer

journal homepage: www.elsevier.com/locate/polymer

EPR study of radical annihilation kinetics of γ -ray-irradiated acrylic (PMMA) at elevated temperatures

Q3 J.S. Peng^a, Li-June Ming^b, Young-Shang Lin^a, Sanboh Lee^{a,*}^a Department of Materials Science and Engineering, National Tsing Hua University, 101 Kuang Fu Road, 2nd Sec., Hsinchu 300, Taiwan^b Department of Chemistry, University of South Florida, Tampa, FL 33620-5250, USA

ARTICLE INFO

Article history:

Received 5 August 2011

Received in revised form

27 October 2011

Accepted 2 November 2011

Available online xxx

Keywords:

Gamma irradiated PMMA

EPR

Thermal annealing

ABSTRACT

High-energy irradiations of polymers may cause bond cleavage or crosslinking and change the structures and physical properties of the polymers, which may offer various applications. Despite wide investigation, relationship between the kinetics and mechanism of annihilation after irradiations and the structure and some physical properties of irradiated polymers is still poorly established. We have been exploring such possible relationship and report herein investigation of the kinetics of radical annihilation of γ -ray irradiated acrylic, i.e., poly(methylmethacrylate) or PMMA, at elevated temperatures with EPR spectroscopy. The EPR spectra consist of three components, a quintet Ra, a quartet Rb, and a broad singlet Rc. Ra and Rb follow second-order annihilation kinetics, while the decay of the radical Rc is comprised of at least two parallel kinetic processes, a slow second-order pathway and a fast pathway which can be equally well fitted to first- or second-order kinetics. The kinetics is analogous to that for the radical decays in irradiated 2-hydroxyethyl methacrylate copolymer. On the basis of the large hyperfine coupling constant of 230 mT, Ra may be assigned to a radical adjacent to two groups of protons, such as a doublet of quartet with similar coupling constants due to an anti-methylene proton and a methyl group; the Rb signal, possibly a methyl radical; and the broad singlet Rc, a magnetically coupled combination species. Alternative assignments of the radicals have also been suggested. The rate constant increases with increasing dose for each radical at a given temperature, possibly due to increase in radical concentrations at higher doses. The rate constants satisfy the Arrhenius equation, suggesting a single mechanistic pathway for the annihilation process in the temperature range; wherein the activation energy decreases with increasing dose for all radicals, possibly due to higher concentrations of free radicals in close proximity produced at higher doses.

© 2011 Published by Elsevier Ltd.

1. Introduction

When polymeric materials are exposed to high-energy irradiations, including UV irradiation, particle bombardment, and γ -ray irradiation, their chemical bonds undergo scission or crosslinking which can drastically change the structures and physical properties of the polymers. Thus, these irradiations may have broad applications, including controlled degradation of synthetic and biopolymers [1–3], influence on optical activities of optical fibers and coatings [4–7], development of color indicators for radiation [8], influence on mechanical properties [4,5], disinfection of bone allografts [9] (despite damages to the bone structure [10,11]) and as a resist in (photo)lithography [12]. Poly(methylmethacrylate)

PMMA or simply “acrylic” is one of the most widely used plastics with unique optical and mechanical properties and has been extensively studied [13], such as its use as an impact-resistant alternative to glass, coating and fiber in optical devices, biocompatible materials in medicine, and painting materials in arts. Irradiated PMMA shows that the bond scissions is affected by the irradiated conditions [14], the mechanical properties are degraded by γ -ray irradiation [15], the average molecular weight [16], the glass transition temperature [17], the micro-hardness [18], and the transmittance [19] decrease with increasing dose of the irradiation while the thermal expansion coefficient increases with increasing dose of irradiation [17], and bond scission takes place when the value of linear energy transfer (LET) was smaller than 15 eV/nm, while crosslinking occurs when greater than 15 eV/nm [20].

Free radicals are the major products in polymeric materials generated by γ -ray irradiation which can be monitored with electron paramagnetic resonance (EPR) spectroscopy. Particularly, the

* Corresponding author. Tel.: +886 3 5719677; fax: +886 3 5722366.

E-mail address: sblee@mx.nthu.edu.tw (S. Lee).

identity of the radicals can be revealed by EPR which renders it possible to characterize the bond scission patterns and annealing kinetics in polymers. We have recently revisited γ -ray irradiated syndiotactic polystyrene (PS) by the use of EPR spectroscopy and kinetics [21], wherein the identity of the radicals was reassigned and the annealing of the radicals at elevated temperatures was found to follow first-order kinetics. However, the annealing kinetics in irradiated 2-hydroxyethyl methacrylate (HEMA) copolymer is quite different, in which two radical components follow second-order kinetics while one has a complex kinetic pathway [22]. Although HEMA and PMMA show some structural similarities, their EPR spectra after irradiation are quite different. Despite extensive investigation of irradiated polymers, relationship between their annihilation kinetics and mechanism and their structure and some physical properties is still poorly established.

The EPR spectrum of irradiated PMMA powder shows apparent two components, a quintet and a quartet, both with a hyperfine coupling constant (hcc) of 260 mT, suggested to be due to the main chain scission radical $-\text{CH}_2\dot{\text{C}}(\text{COOMe})\text{CH}_3$ [23,24]. A nine-line EPR spectrum in irradiated PMMA was assigned to the monomer radical and a chain ending radical [25], independent of the presence of 2.5% squalene [26]. Therein, the decay of radicals in a sample of 1-mm thick was faster than that of 2-mm sample, which however cannot be due to the intrinsic decay of the radicals yet attributable to oxygen and free radical diffusion [26]. Further EPR studies of irradiated PMMA powder at 77 K [27] revealed three types of radicals, suggested to be $-\dot{\text{C}}\text{H}-$, $-\text{COO}\dot{\text{C}}\text{H}_2$, and the anion radical $-\dot{\text{C}}(\text{O}^-)\text{OCH}_3$ which were also suggested to be in irradiated poly(ethylmethacrylate) at 77 K [28]. Moreover, we observed a broad single-line signal in PMMA irradiated with dose greater than 320 kGy [29]. Further studies with GPC and EPR suggested the efficiency of main-chain scission decreased with decreasing temperature below 200 K and was constant above 200 K [30]. In this article we report the study of γ -ray irradiated PMMA by the use of EPR spectroscopy, wherein a few radicals were detected and identified and their decays analyzed with kinetics, and correlation with other physical properties further discussed.

2. Experimental

PMMA was obtained from Dupont, DE, as 6.35-mm thick Lucite L type cast acrylic sheet. The specimens were cut from the PMMA sheet into $4.0 \times 5.0 \times 20 \text{ mm}^3$, ground with 800, 1200, and 4000 carbimet papers, and polished with $1.0 \mu\text{m}$ alumina slurries. Then the specimens were annealed at 368 K in air and furnace cooled to room temperature for 24 h, then sealed in glass in air and irradiated by a Co^{60} γ -ray source with dose rates 16 kGy/h at room temperature. The doses were 320, 480, 640 and 840 kGy.

EPR spectra were recorded at 298 K using a Bruker EMX-10 EPR spectrometer (Kahrslule, Germany) with a dual cavity. The microwave power, modulation amplitude, time constant and scan range are 20.02 mW, 16 mT, 81.92 ms, and 2 T, respectively. The EPR spectrum of each specimen was measured immediately after irradiation, annealing at 313, 323, 333, 343, and 353 K. The EPR spectrum of a specimen was measured in one cavity port, while the corresponding EPR spectrum of DPPH (2,2-diphenyl-1-picrylhydrazyl) standard with a total spin of 2.0×10^{15} was recorded under the same conditions in the other port. Each EPR spectrum was first deconvoluted into a minimum number of components that afford good overall simulation by the use of the software WinSim2002 [31] (NIEHS–NIH). Then, each derivative-like EPR component from the deconvolution was double integrated to afford the signal area as the signal intensity and compared with that of the DPPH standard to yield the number of spins. The spins of the deconvoluted components are then fitted to an appropriate rate law to reveal the kinetic

pattern for the decay. The use of 20 mW increases the signal intensity by about two times relative to that of 2.0 mW which allows clear detection of signal decay for a long period of time up to more than four days. Otherwise, a four times of the number of scans would be needed to achieve the same signal-to-noise ratio acquired with 2 mW, which would not be practical especially for acquiring the spectra at the beginning when the decay is relatively faster. The high microwave power results in $\sim 30\%$ saturation and an overestimate of the rate constant k which can be easily calibrated. Nevertheless, the reaction order and the activation energy for the decay from the slope of $\log(k)$ -vs.- $1/T$ plots are not affected.

3. Results and discussion

3.1. EPR spectral features

The EPR spectra of annealed PMMA irradiated with γ -ray at doses of 320, 480, 640, and 800 kGy at room temperatures are virtually identical and a prototypical one with 320 kGy irradiation dose is presented (Fig. 1). The similarity indicates that the generation and the decay of radicals reach equilibrium during the irradiation with the various doses. The spectra in a wide range of temperature from liquid nitrogen temperatures to 353 K are alike, which indicates that the line-broadening may not be due to increase in electronic relaxation and/or dynamic fluxion or mobility but may be due to inhomogeneity of the radical environment in the polymer. The spectra, however, are significantly different from those of irradiated syndiotactic PS [21] and HEMA copolymer [22], despite the presence of similar functional groups in HEMA and PMMA (Fig. 1). The spectrum of irradiated PMMA shows a significantly larger hcc and spin multiplicity than those of PS and HEMA, indicating the production of different types of free radicals from the latter ones. Since optical and mechanical properties of polymers are affected by high-energy irradiations, it is thus important to identify the radicals and understand the polymer chain cleavage patterns rendered by the irradiations and correlation with the structures of the polymers.

The EPR spectra of PMMA irradiated with 320 kGy and annealed at 313 K right after the irradiation (Fig. 2A) and 10 h later (Fig. 2B) have very different features, showing a distinct broad signal with small amounts of sharper features at a longer annealing time. The spectral features are also different from samples irradiated with a low dose of 5.0 kGy in the dark at 77 K [27,28] since only stable radicals can be detected at the elevated temperatures. Despite their

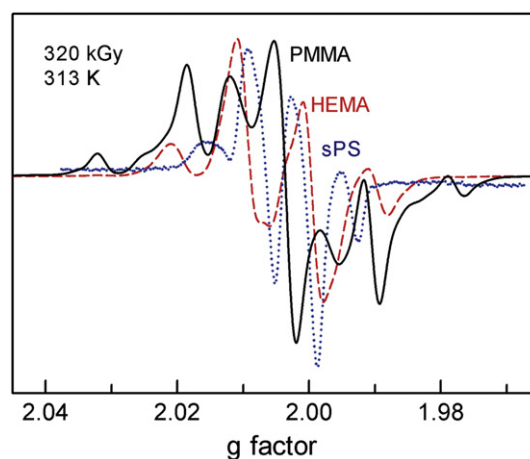


Fig. 1. EPR spectra of γ -ray irradiated (320 kGy) PMMA (solid trace), HEMA copolymer (dashed trace), and PS (dotted trace) at 313 K.

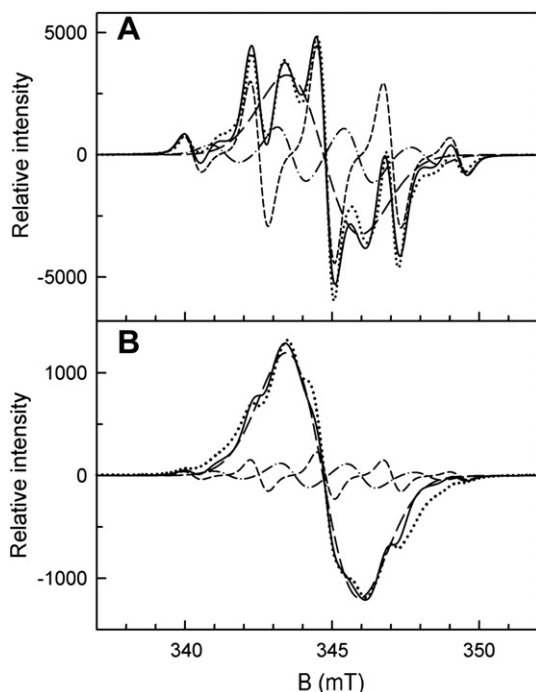


Fig. 2. EPR spectra (dotted traces) of PMMA irradiated with 320-kGy γ -ray and annealing at 313 K immediately (A) and after 10 h (B). The spectra are deconvoluted into radicals Ra (dashed traces), Rb (dash-dotted traces), and Rc (long-dash traces), along with the simulated spectra (solid traces) from these three components.

different features, the spectra at the different annealing times at 313 K can be deconvoluted into the same three components (Fig. 2 and Table 1). One component is a quintet with intensity ratio 1:4:6:4:1 (short dashed traces) dubbed radical Ra, another component is a quartet with intensity 1:3:3:1 (dashed-dotted trace) dubbed radical Rb, and the third component is a broad singlet signal (long dashed trace) dubbed Rc. The simulated spectra (solid traces, Fig. 2) with the three components are in good agreement with the experimental spectra. The significant decrease in the signal intensity of Ra and Rb with time reflects their lower stability. Moreover, the same hcc of 230 mT in Ra and Rb is close to previously reported [23,24] yet significantly higher than those in irradiated PS (<125 mT) [21] and HEMA (170 mT) [22], reflecting different proton environment around the radical which is further discussed below.

3.2. Bond cleavage and assignment of EPR signals

There are four possibilities for bond breakage to occur in PMMA on the main chain to produce a tertiary radical and a methylene radical (Scheme 1, pathways *a* and *a'*), on the side chain to produce a methyl radical and a tertiary radical with two adjacent methylene groups (*b*), and on the carboxyl side chain to yield a methyl group

Table 1
Isotropic EPR parameters^a of the radicals yielding spectra of PMMA in Fig. 1.

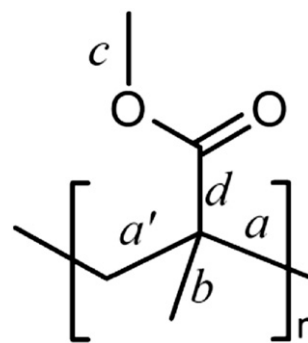
Radical	g-factor	pattern	N ^b	A/mT ^c	$\Delta H/mT^d$
Ra	2.0036 (2)	1:4:6:4:1	4	230 (20)	60
Rb	2.0032 (2)	1:3:3:1	3	230 (20)	100
Rc	2.0042 (2)	1	—	—	250

^a The numbers in parentheses are the estimated standard deviation.

^b Number of adjacent equivalent protons.

^c Hyperfine coupling constant.

^d Peak to peak linewidth of individual line.



Scheme 1.

and a carboxyl group (*c*) or a tertiary radical and a methylcarboxyl radical (*d*). An early study of γ -ray irradiated PMMA by the use of mass spectrometry revealed the production of relatively large molar amounts of CO (30.5%), CO₂ (15.7%), CH₄ (13.1%), and HCOOCH₃ (14.2%) and some HCHO (3.0%) [32], suggesting a predominant bond cleavage at (*d*), and possibly (*b*) as well, as the primary or a secondary process. Moreover, the nine-line spectrum was suggested to be attributed from the main chain scission radical $-\dot{C}H_2(COO)CH_3$ resulted from the decay of the side-chain $-\dot{C}OOC H_2$ radical [27,28], wherein the methyl group shows a hcc ca. 230 mT and the two methylene protons have their distinction coupling constants [33].

The quintet with a large hcc of the radical Ra may arise from a free radical with 4 equivalent protons, possibly originated from (i) a tertiary radical adjacent to four equivalent protons or (ii) a doublet of quartet with nearly identical hcc's. In the case (i) via the cleavage pattern (*b*), a tertiary radical is formed wherein only those protons at the *syn* or *anti* position on an adjacent carbon to the free radical can afford large hcc's in the magnitude of ~ 230 mT in rigid configurations, analogous to the Karplus correlation commonly used for the explanation of the J coupling in NMR [34] and for the explanation of the coupling between a radical orbital and a beta-H [35]. Since only one proton on each methylene group can be at the *syn* or *anti* position, spin multiplicity of a triplet or less with the large hcc would be seen. Conversely, a quintet can be seen when this radical moiety has fast motion to average out the different configurations of the adjacent methylene protons. However, since the EPR spectra are not much sharper at elevated temperatures than at liquid nitrogen temperatures, restriction of rotation may be the case in this polymer. Cleavage of the main chain (*a* or *a'*) yields a tertiary radical that is adjacent to a methyl and a methylene group as in the case (ii), and was previously suggested [27,28,35]. In this case, the polymer chain must adopt a rigid configuration wherein one of the methylene protons is nearly at the *anti* position with respect to the radical, whereas the methyl group at the vicinal position to a radical can afford a coupling constant in a large range of ~ 130 – 230 mT [36], depending on the neighboring functional groups [37,38], and is ~ 230 mT in *t*-butyl radical and several hydrocarbon radicals [36,39]. If main-chain cleavage occurs, a spin-triplet secondary radical is expected to form as $\bullet CH_2-C(CH_3)(COOCH_3)-$. Since there is no significant contribution from spin triplet in the deconvoluted spectra, it is possible that this radical is quenched by decarboxylation and formation of a double bond. The decarboxylation was suggested to be one main pathway in irradiated PMMA [32].

This quintet signal of Ra with a large hcc marks a significant difference between PMMA and the analogous HEMA copolymer of 170 mT [22] as well as PS of <125 mT [21]. A common structural feature between PMMA and HEMA is the backbone repeats of $-\dot{C}H_2CR(CH_3)-$ with R = $-\text{COOCH}_2\text{CH}_2\text{OH}$ in HEMA and $-\text{COOCH}_3$

in PMMA. However, the backbone is the most probable cleavage in PMMA to afford the hcc of 230 mT. The lack of a quintet radical component thus reflects possible resistance in backbone cleavage in HEMA, which might be attributable to its structural rigidity due to crosslinking and/or relatively more cleavage-prone side chains.

The 1:3:3:1 quartet of the radical Rb can be originated from (iii) a radical hyperfine-coupled with three equivalent protons or (iv) a methylcarboxyl radical. However, the latter (iv) is not expected to exhibit a large hcc since the methyl is separated from the radical by an O atom. The production of CH₄ observed in γ -ray irradiated PMMA [32] reflects the generation of methyl radical (via *b* or *c*) that follows by proton extraction. The hcc of a methyl radical trapped in methane matrix at 4.2 K was previously determined to be 230 mT [40], consistent with the hcc measured herein. Since the kinetics for the generation of CH₄ was not determined therein to match with the decay of Rb radical, the identity of this quartet although consistent with a methyl is tentative. An allylic radical with the resonance structures of [\bullet CH₂-C(COOCH₃)=CH- \leftrightarrow CH₂=C(COOCH₃)- \bullet CH-] can be formed via proton extraction of an alkene moiety formed during irradiation which was suggested to exhibit a spin quartet due to the three nearly equivalent protons [35]. However, the hcc's for the allylic protons are around or less than 150 mT [41], too small to be accounted for the observed quartet herein. Alternatively, generation of a double bond on the polymer main chain as -CH=C(COOCH₃)-CH₂- and its attack by a methyl radical may form a tertiary radical in the form of -CH(CH₃)- \bullet C(COOCH₃)-CH₂- which would give a quartet. In this case, the bonds around the radical need to be fluxional to average out the β -CH and β -CH₂ proton hyperfine couplings to afford a quartet.

The broad singlet signal of Rc has a *g*-factor 2.0042 and a large peak-to-peak linewidth of 250 mT. The lack of significant hcc's of this singlet reflects that it is a radical isolated from protons, such as a radical generated from the carboxyl group. The broadness of this signal does not seem to be consistent with those of Ra and Rb radicals, possibly due to a combination of more than one species and/or a significantly lower T₂ relaxation. Rc is observed in PMMA with γ -ray irradiation dose greater than 320 kGy [19], but not lower than that dose. Thus, it is also probably resulted from magnetic coupling due to multiple adjacent radicals that are likely to be generated at higher irradiation doses. The irradiated HEMA copolymer also exhibits a broad EPR feature [22]. Since a common structural feature between PMMA and HEMA that lacks interaction with protons is the carboxyl group, this radical Rc is thus possibly partially attributed to bond breakage on the carboxyl side chains. The identity of these radicals cannot be fully assigned without selective isotope labeling on the protons (with deuterium atoms) and/or carbons (with ¹³C), which await future exploration.

Correlation with photodegradation of PMMA caused by pulsed laser UV irradiation can be drawn, wherein cleavages on the mainframe (pathways *a* or *a'* in Scheme 1) and side chains (*b*, *c*, and *d*) are suggested along with the rearranged secondary radicals by means of EPR, mass spectrometry, and IR spectroscopy [42]. Mechanism for the photolysis and formation of various radicals therein was proposed. However, the kinetics for the decay of the radicals has never been determined. Since PMMA is commonly used as a resist in the (photo)lithography process with an electron beam, far UV, or X-ray [12], which results in chain scission and bond cleavage and can afford high-resolution nanostructures [43,44], better understanding of the kinetic of its lithographic process with high-energy beams and subsequent annihilation is thus expected to provide insights into structure-reactivity correlation for further applications in nanotechnology. Time-dependent changes of the radical spin numbers were thus determined to reveal the rate laws and rate constants for the decays.

3.3. Kinetics of radical decays

The double integral of each sub-spectrum is proportional to the spin number of the corresponding radical, which can be quantified with respect to the DPPH standard of 2×10^{15} spins in 420 mm³ and the spin concentrations of Ra, Rb, and Rc obtained by the corresponding spin number divided by volume. The spin concentration of Ra as a function of time at temperatures 313–353 K for doses 320 kGy are plotted in Fig. 3A. The traces obtained for 480, 640 and 800 kGy are similar. Likewise, the decays of spin concentrations of Rb and Rc are shown in Fig. 3B and C, respectively. The spin concentration decreases with increasing annealing time for all temperatures regardless of the irradiation dosage. For a given time and dose, the spin concentration increases with decreasing temperature. The change in the spin concentrations *N*'s of Ra and Rb was analyzed with kinetic models, and was found to be best fitted to a second-order kinetic process (Eq. (1)),

$$\frac{dN}{dt} = -k_2 N^2 \quad (1)$$

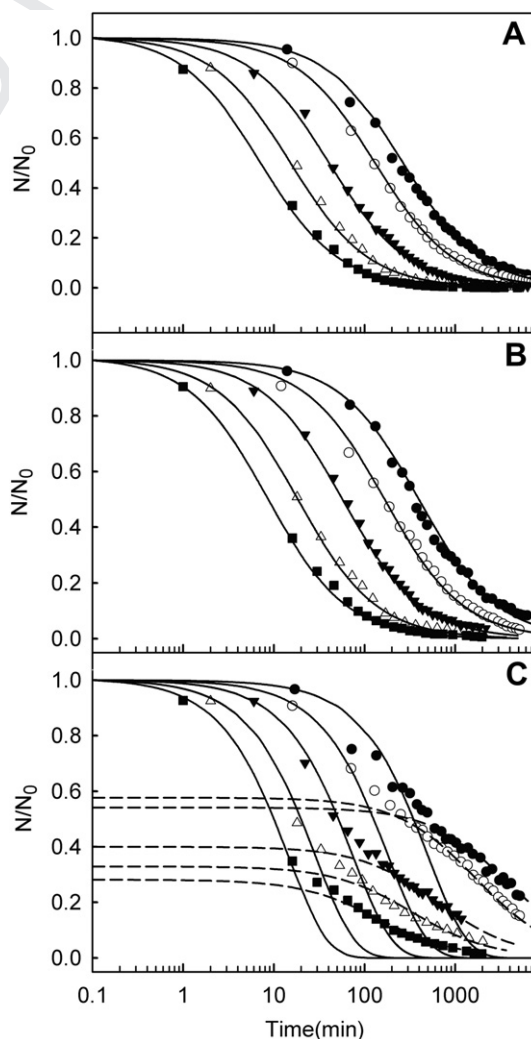


Fig. 3. The spin concentration of radicals Ra (A), Rb (B), and Rc (C) as a function of time at 313 (●), 323 (○), 333 (▼), 343 (△), and 353 (■) K with irradiation dose of 320 kGy. The decays of the radicals obtained at different doses of 480, 640, and 800 kGy behave similarly. The dashed and solid traces in C are best fits to Eqs. (2) and (4), respectively.

wherein k_2 is the second-order rate constant. The solution of Eq. (2) is

$$1/N = k_2 t + 1/N_0 \quad (2)$$

wherein N_0 is the initial spin concentration. The data are poorly fitted to a first-order kinetic pathway.

The solid traces in Fig. 3A and B are the best fit of the decay of the radicals Ra and Rb to Eq. (2), where the initial concentrations are listed in Table 2 and the values therein in parentheses are experimental data. The calculated N_0 values are always greater than the experimental data for all temperatures and doses because the spin concentration decays very fast at a short time that may result larger error than at a longer time. Moreover, there is a short initial delay between the end of the irradiation and the EPR spectral acquisition. Nevertheless, the rate constants are not changed by the initial delay and the N_0 values.

The temperature-dependence of the rate constants for the decay of the spin concentrations of the radicals satisfies the Arrhenius equation as shown in Fig. 4, from which the activation energy can be obtained as 77–80 kJ/mol for Ra and 82–85 kJ/mol for Rb (Table 3). The activation energy decreases with increasing dose for both radicals Ra and Rb. This may be attributed to the fact that higher concentrations of free radicals in close proximity can be produced at higher doses which results in easier termination of free radicals through coupling of proximal radicals. For a given dose, the activation energy of Ra is slightly smaller than that of Rb. It is probably due to that a methylene radical (Ra) is easier than a methyl radical (Rb) to recombine with cleaved polymer chain. On the basis of the experimental observations, there is a kinetic barrier that prevents the annihilation of the radicals. It is known that radicals in polymers formed by various methods can be quite stable owing to the relative rigidity of the polymer chains in the condensed phase which affords only limited mobility. The nature of this activation energy is thus not attributable to bond breakage but due to physical restriction of an isolated radical to pair up with another radical or rearrange to afford unsaturated bond. Bimolecular reactions are suggested to follow second-order kinetics in condensed phases when the reactions simply need to overcome the activation barrier upon collision, which are supposed to show Arrhenius equation-like behavior [45,46]. The kinetics observed

Table 2

The initial spin concentration N_0 of radicals Ra, Rb, and Rc and \bar{N} of radical Rc of PMMA with different doses and annealing temperatures. The values in parentheses are experimental data of initial concentration.

ϕ (kGy)	T (K)	N_0		\bar{N}	
		$R_a (\times 10^{17})$	$R_b (\times 10^{17})$	$R_c (\times 10^{18})$	$R_c (\times 10^{17})$
320	313	3.95 (3.77)	3.6 (3.46)	1.2 (1.16)	6.5
	323	4.5 (4.05)	4.3 (3.90)	1.3 (1.18)	7.5
	333	5.25 (4.50)	4.75 (4.22)	1.3 (1.20)	5.2
	343	5.1 (4.46)	5.0 (4.47)	1.4 (1.29)	4.6
	353	4.8 (4.14)	4.55 (4.07)	1.25 (1.15)	3.5
480	313	4.1 (3.93)	4.1 (3.91)	1.42 (1.37)	7.6
	323	4.3 (3.90)	4.2 (3.90)	1.45 (1.39)	10.0
	333	4.3 (3.66)	4.05 (3.61)	1.6 (1.34)	7.0
	343	4.7 (4.01)	4.7 (3.97)	1.7 (1.46)	5.5
	353	3.6 (3.03)	3.5 (3.07)	1.42 (1.08)	3.7
640	313	3.8 (3.24)	3.55 (3.16)	1.62 (1.31)	8.0
	323	4.45 (3.60)	4.3 (3.45)	1.75 (1.48)	9.5
	333	4.7 (3.61)	4.9 (3.47)	1.55 (1.49)	6.5
	343	4.2 (3.47)	4.4 (3.45)	1.28 (1.39)	4.5
	353	3.7 (3.03)	3.7 (3.01)	1.5 (1.18)	5.0
800	313	3.7 (3.38)	3.5 (3.24)	1.5 (1.44)	9.0
	323	4.8 (3.78)	4.4 (3.60)	1.7 (1.56)	10.0
	333	4.2 (3.41)	4.0 (3.18)	1.55 (1.45)	6.5
	343	4.5 (3.57)	4.4 (3.31)	1.76 (1.61)	5.1
	353	3.6 (2.96)	3.95 (3.01)	1.4 (1.25)	4.0

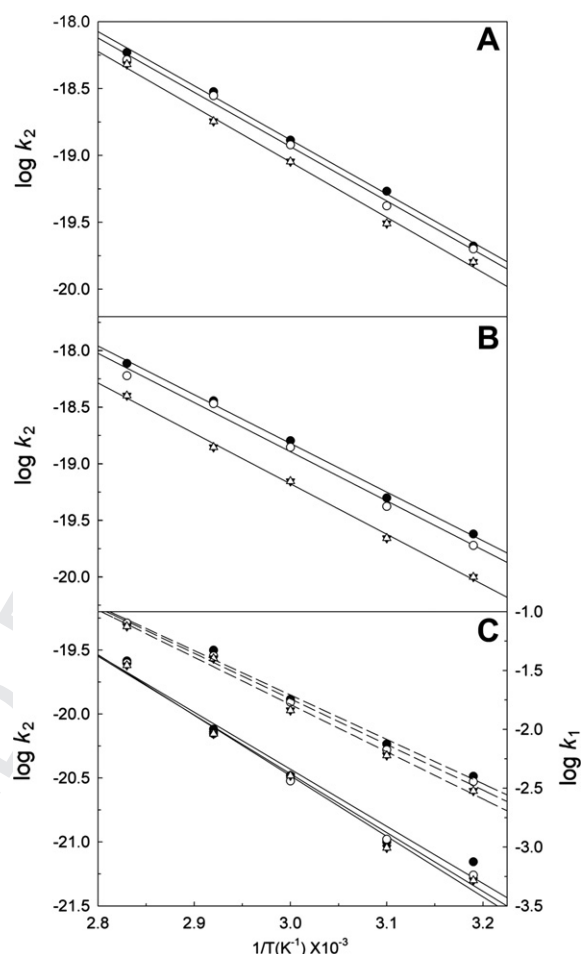


Fig. 4. Arrhenius plots of the rate constants for the annihilation of radicals Ra (A), Rb (B), and Rc (C) irradiated with 320 (Δ), 480 (\blacktriangledown), 640 (\circ), and 800 (\bullet) kGy. The solid and dashed lines are obtained for the slow and fast decays of radical Rc, respectively.

herein fits this pattern. However, different systems can behave differently, even among polymers that show first-order or second-order annihilation process as we previously observed [21,22]. We also experienced that the annihilation of color centers in LiF single crystals was too complicated to be analyzed on the basis of a thermally activated process [47]. Moreover, the annealing in other cases such as semiconductors is also chemically and physically different process from radical annihilation of irradiated polymers [48].

The attenuation of spin concentration of radical Rc cannot be adequately fitted to 1 s-order kinetic process shown in Eq. (2) as for Ra and Rb. However, the data can be deconvoluted and well fitted to a two-step decay process, with a faster step following first-order kinetics (solid traces, Fig. 3) shown in Eq. (3) and a slower step following second-order kinetics (dashed traces, Fig. 3),

Table 3

The activation energies (kJ/mol) for the decay of radicals Ra, Rb and Rc of irradiated PMMA.

Radical	Dose (kGy)			
	320	480	640	880
Ra	80.5 \pm 3.7	78.5 \pm 4.1	77.3 \pm 3.1	77.1 \pm 1.2
Rb	85.2 \pm 4.7	83.9 \pm 3.2	82.8 \pm 4.5	81.9 \pm 3.4
Rc (fast step)	82.4 \pm 1.6	76.5 \pm 3.6	73.8 \pm 3.5	71.8 \pm 3.8
Rc (slow step)	91.0 \pm 5.5	90.0 \pm 7.0	87.2 \pm 7.0	84.6 \pm 9.2

$$\frac{dN}{dt} = -k_1 N \quad (3)$$

wherein k_1 is the first-order rate constant. The solution of Eq. (3) is shown in Eq. (4),

$$N = N_0 \exp(-k_1 t) \quad (4)$$

wherein N_0 is the initial spin concentration. Note that the concentration for the slower step is the normalized concentration (\bar{N}), which is different from N_0 during fitting to Eq. (2) (Table 2). The fast decay can be equally fitted with a second-order decay. However, owing to the limited number of data points, differentiation between the two reaction orders for the fast initial decay cannot be made and a fast first-order is modeled and presented herein. The temperature-dependence of the rate constants was fitted to the Arrhenius equation to afford the activation energies (72–82 kJ/mol for the faster step and 85–91 kJ/mol for the slower step; Table 3) which decreases with increasing dose. It is also found that for a given dose the activation energy follows the sequence $R_a < R_b < R_c$ in the range of 77–91 kJ/mol for the second-order kinetics. The relatively high activation energy of R_c compared to those of R_a and R_b results in its much longer life time, which renders R_c to be the predominant radical form after annihilation for 10 h (Fig. 2B). The fast first-order kinetics is observed only in radical R_c . It is probable that it is either too fast to be observed or not present at all in radicals R_a and R_b .

3.4. Irradiations and physical/mechanical properties

The color of PMMA changes to yellow or brown upon γ -ray irradiation. Since PMMA is transparent to the visible light, the appearance of color centers must be attributed to defects that absorb visible light. The formation of color centers in irradiated PMMA with irradiation dose from 400 to 1000 kGy was reported to also follow a second-order kinetic process [19]; however, with activation energies in the range of 44–51 kJ/mol that are significantly different from those for the decays of the radicals observed herein. It implies that the formation of the color center is not directly attributed to the decay of radicals. Moreover, hardness of PMMA was found to decrease linearly with radiation-induced defects and increase with increasing time during isothermal annealing [18]. Therein, the increase in hardness due to annihilation of the defects follows a first-order kinetic process with activation energies within 36–45 kJ/mol in the dose range of 400–1000 kGy. Because the annihilation of the defects and the formation of the color centers have different reaction orders and lower activation energies from those of the decays of the radicals (Table 3 and Fig. 3), both the hardening due to the defects and the transmittance due to coloration occur with lower activation energies (hence faster rates) which are thus not likely to be directly attributed to the decay of radicals in the range of the experimental time although they might be linked to processes associated with radical decays. The hardening and coloration with faster rates may most probably take place prior to the radical decays in the time frame we monitored.

Although the change in physical properties can be associated with the formation or decay of free radicals (such as EPR spectral features and intensities due to the identity and quantity of radicals, change in hardness due to bond breakage or crosslinking, and detection of color centers due to formation of defects), the changes occurring outside the time frame of the radical decays herein would not be detected. The different rate constants of some physical properties from those of the radical decays herein suggest their different mechanisms and/or time frames during γ -ray irradiation. A recent study showed that pure PMMA film has no influence on its

UV/Vis spectrum upon UV irradiation [49]. However, the use of low-intensity Hg UV lamp for the study may not effectively cause bond-cleavage reactions in the polymer. Conversely, the two peaks at 270 and 315 nm in PMMA disappear after γ -ray irradiation and the intensity in the UV/Vis range decreases with increasing irradiation time [19].

4. Summary and conclusion

After irradiated with γ -ray, PMMA exhibits EPR spectra attributed to at least three radicals R_a , R_b , and R_c . The radicals R_a and R_b are attributed to the cleavage of the main chain and the side chains. R_c has a broad single-line spectra which is probably attributed to the presence of magnetic coupling between/among radicals in close proximity. For a given dose and temperature, the spin concentration of each radical decreases with time. With the exception of radical R_c in a short-time period that follows a fast annihilation process, the slower decays of the radicals can be fitted by a second-order annihilation process. The complicated nature of R_c decay also reflects that it may be a combination of multiple magnetically coupled species. For all the decays, the rate constants satisfy the Arrhenius equation from which the activation energies are obtained. The color center related to transmittance of irradiated PMMA also follows a second-order kinetic process, but with much lower activation energies [19]. However, the hardness controlled by the defects created by irradiation is governed by a first-order annihilation process and rate constants [18]. These observations imply that the color centers and the defects are not directly attributed to the decay of radicals R_a , R_b , and R_c in the range of the experimental time.

Acknowledgment

This work was supported by the National Science Council, Taiwan (SL). Support by the National Science Foundation, USA, to L-JM (CHE-0718625) is also acknowledged.

References

- [1] Chung HJ, Liu Q. Effect of gamma irradiation on molecular structure and physicochemical properties of Corn starch. *J Food Sci* 2009;74:C353–61.
- [2] Lotfy S. Controlling degradation of low-molecular-weight natural polymer "dextrin" using gamma irradiation. *Int J Biol Macromol* 2009;44:57–63.
- [3] De Kerf M, Mondelaers W, Lahorte P, Vervaeck C, Remon JP. Characterisation and disintegration properties of irradiated starch. *Int J Pharmaceu* 2001;221:69–76.
- [4] El-Farahaty KA, Sadik AM, Hezma AM. γ -Irradiation effects on opto-thermal and -mechanical properties of PET and PETG fibers. *Int J Polym Mater* 2009;58:366–83.
- [5] Aghamiri SMR, Namedanian M, Sanjabi Z. Effect of gamma irradiation on the light polarization variation of PMMA polymer. *Opti Commun* 2008;281:356–9.
- [6] Medhat M, El-Zaiat SY, Abdou SM, Radi A, Omar MF. Interferometric determination of gamma radiation effects on optical parameters of a GRIN optical fibre. *J Opti A Pure Appl Opti* 2002;4:485–90.
- [7] Fouda IM, Shabana HM. Opto-mechanical properties of fibres. Part 3. Structural characterization of uniaxial orientation in drawn poly(ethylene terephthalate) by means of optical parameters. *Polym Int* 1999;48:198–204.
- [8] Hatada M, Sakamoto Y, Katanosaka A. Coloration of pentacosadiynoic acid polycrystalline powder dispersed in polymer layer by gamma-ray irradiation and UV illumination. *J Photopolym Sci Technol* 2002;15:741–7.
- [9] Campbell DG, Li P, Stephenson AJ, Oakeshott RD. Sterilization of HIV by gamma irradiation. A bone allograft model. *Int Orthop* 1994;18:172–6.
- [10] Currey JD, Foreman J, Laketic I, Mitchell J. Effects of ionizing radiation on the mechanical properties of human bone. *J Orthop Res* 1997;15:111–7.
- [11] Akkus O, Rimnac CM. Fracture resistance of gamma radiation sterilized cortical bone allografts. *J Orthop Res* 2001;19:927–34.
- [12] Bowden MJ. A perspective on resist materials for fine-line lithography. In: Thompson LF, Willson CG, Fréchet JM, editors. *Materials for Microlithography* (ACS Symposium Series 266). Washington DC: ACS; 1984 [Chapter 3].
- [13] Masson J. Acrylic fiber technology and applications. Marcel Dekker; 1995.
- [14] Wall LA, Brown DW. Gamma irradiation of polymethyl methacrylate and polystyrene. *J Phys Chem* 1957;61:129–36.

- [15] Kudoh H. Application of target theory for the radiation degradation of mechanical properties of polymer materials. *J Mater Sci Lett* 1996;15:666–9.
- [16] Ouano AC, Johnson DE, Dawson B, Pederson LA. Chain scission efficiency of some polymers in gamma-radiation. *J Polym Sci A Polym Chem* 1976;12:701–11.
- [17] Subrahmanyam HN, Subrahmanyam SV. Thermal-expansion of irradiated poly(methyl methacrylate). *Polymer* 1987;28:1331–3.
- [18] Lu KP, Lee S, Cheng CP. Hardness of irradiated poly(methyl methacrylate) at elevated temperatures. *J Appl Phys* 2001;90:1745–9.
- [19] Lu KP, Lee S, Cheng CP. Transmittance in irradiated poly(methyl methacrylate) at elevated temperatures. *J Appl Phys* 2000;88:5022–7.
- [20] Lee EH, Rao GR, Mansur LK. LET effect on cross-linking and scission mechanisms of PMMA during irradiation. *Radiat Phys Chem* 1999;55:293–305.
- [21] Lin C-C, Ming L-J, Lee C-C, Lee S. EPR kinetics in irradiated syndiotactic polystyrene at elevated temperatures. *Polymer* 2008;49:3987–92.
- [22] Lin Y-S, Ming L-J, Peng JS, Fu Y-K, Lee S. Radical annihilation of gamma-Ray-irradiated contact lens blanks of 2-Hydroxyethyl methacrylate copolymer at elevated temperatures. *J Appl Poly Sci* 2010;117:3114–20.
- [23] Abraham RJ, Melville HW, Ovenall DW, Whiffen DH. Electron spin resonance spectra of free radicals in irradiated polymethyl methacrylate and related compounds. *Trans Faraday Soc* 1958;54:1133–9.
- [24] Ingram DJE, Symons MCR, Townsend MG. Electron resonance studies of occluded polymer radicals. *Trans Faraday Soc* 1958;54:409–15.
- [25] Piette LH. NMR and EPR spectroscopy. Varian associates. London: Pergamon Press; 1960 ([Chapter 17]).
- [26] Trihi M, Duroux JL, Hyvernaud MJ, Bernard M. Study of free radicals in irradiated PMMA (doped or undoped) using ESR spectroscopy. *Appl Radiat Isot* 1996;47:1561–3.
- [27] Ichikawa T, Yoshida H. Mechanism of radiation-induced degradation of poly(methyl methacrylate) as studied by ESR and electron spin echo methods. *J Polym Sci A Polym Chem* 1990;28:1185–96.
- [28] Tanaka M, Yoshida H, Ichikawa T. Thermal and photo-induced reactions of polymer radicals in γ -irradiated Poly(alkyl methacrylate). *Polym J* 1990;22:835–41.
- [29] Lin YS, Lee S, Lin BC, Cheng CP. EPR studies of high dose gamma-irradiated poly(methyl methacrylate). *Mater Chem Phys* 2003;78:847–51.
- [30] Ichikawa T, Oyama K-I, Kondoh T, Yoshida H. Efficiency of radiation-induced main-chain scission of poly (methyl methacrylate) depends on the irradiation temperature because of coexisting monomer. *J Polym Sci A Polym Chem* 1994;32:2487–92.
- [31] Duling DR. Simulation of multiple isotropic spin trap EPR spectra. *J Magn Res B* 1994;104:105–10.
- [32] Todd A. The mechanisms of radiation-induced changes in vinyl polymers". *J Polym Sci* 1960;42:223–47.
- [33] Hill DJT, O'donnel JH, Pomery PJ, Saadat G. Degradation of poly(2-hydroxyethyl methacrylate) by gamma irradiation. *Radiat Phys Chem* 1996;48:605–12.
- [34] Levitt MH. Spin dynamics: basics of nuclear magnetic resonance. Chichester: Wiley; 2008 [Chapter 3].
- [35] Bullock AT, Sutcliffe LH. E.s.r. spectra of free radicals derived from poly-methylmethacrylate. *Trans Faraday Soc* 1964;60:625–33.
- [36] Jay K, Kochi JK, Krusic PJ. Electron spin resonance of Aliphatic hydrocarbon radicals in solution. *J Am Chem Soc* 1968;90:7155–7.
- [37] Fielding AJ, Franchi P, Roberts BP, Smits TM. EPR and computational studies of the formation and beta-scission of cyclic and acyclic dialkoxylalkyl radicals. *J Chem Soc Perkin* 2002;2:155–63.
- [38] Turro NJ, Lei X-G, Jockusch S, Li W, Liu Z, Abrams L, et al. EPR investigation of persistent radicals produced from the photolysis of dibenzyl ketones adsorbed on ZSM-5 zeolites. *J Org Chem* 2002;67:2606–18.
- [39] Wood DE, Sprecher RF. E.P.R. evidence for the non-planarity of t-butyl radical. *Mol Phys* 1973;26:1311–6.
- [40] Zhitnikov RA, Dmitriev YA. Detection of free radicals in low-temperature gas-grain reactions of astrophysical interest. *Astro Astrophys* 2002;386:1129–38.
- [41] Kochi JK, Krusic PJ. Isomerization and electron spin resonance of allylic radicals. *J Am Chem Soc* 1968;90:7157–9.
- [42] Gupta A, Liang R, Tsay FD, Moacanin J. Characterization of a dissociative excited state in the solid state: photochemistry of Poly(methyl methacrylate). *Photochemical processes in polymeric systems. Macromolecules* 1980;13:1696–700.
- [43] Hoole ACF, Welland ME, Broers AN. Negative PMMA as a high-resolution resist—the limits and possibilities. *Semicond Sci Technol* 1997;12:1166–70.
- [44] Oehrlein GS, Phaneuf RJ, Graves DB. Plasma-polymer interactions: a review of progress in understanding polymer resist mask durability during plasma etching for nanoscale fabrication. *J Vacu Sci Technol B* 2011;29: 010801.
- [45] Waite TR. General theory of bimolecular reaction rates in solids and Liquids. *J Chem Phys* 1958;28:103–6.
- [46] Waite TR. Bimolecular reaction rates in solids and liquids. *J Chem Phys* 1960;32:21–3.
- [47] Lin HY, Tsai YZ, Lee S. *J Mater Res* 1992;7:2833–9.
- [48] Brown WL, Waite TR. Annealing of radiation defects in semiconductors. *J Appl Phys* 1959;30:1258–68.
- [49] Zidan HM, El-Khodary A, El-Sayed IA, El-Bohy HI. *J Appl Polym Sci* 2010;117: 1416–23.